NÖHÜ Müh. Bilim. Derg. / NOHU J. Eng. Sci., 2025; 14(1), 271-281

Niğde Ömer Halisdemir Üniversitesi Mühendislik Bilimleri Dergisi
Niğde Ömer Halisdemir University Journal of Engineering Sciences

Araştırma makalesi / Research article

www.dergipark.org.tr/tr/pub/ngumuh / www.dergipark.org.tr/en/pub/ngumuh

# Grid interconnection solutions and power quality enhancement for a battery-supported hybrid PV system

## Batarya destekli bir hibrit PV sistemi için şebeke bağlantı çözümleri ve güç kalitesinin iyileştirilmesi

**Batuhan Güzey[1,*], Helin Bozkurt[2], Ahmet Teke[3]**

[1] *Aselsan, Ankara, Türkiye*
[2] *Tarsus Universitesi, Elektrik Elektronik Mühendisliği Bölümü, Tarsus,Mersin, Türkiye*
[3] *Çukurova Üniversitesi, Elektrik Elektronik Mühendisliği Bölümü, Balcalı, Adana, Türkiye*

**Abstract**

The energy demand is increasing unprecedentedly day by day due to the rapid development of technology. Clean and sustainable energy sources are used more intensively to meet environmental demands. This paper aims to design a grid-connected hybrid system consisting of a 12.45 kW Photovoltaic (PV) system and a 10 kWh capacity battery energy storage system (BESS). In the design procedure, Perturb and Observe (P&O), Incremental Conductance (INC), Artificial Neural Network (ANN), and Hybrid Maximum Power Point Tracking (MPPT) algorithms are implemented and tested. The most efficient method is selected to yield the maximum power output from the PV module under a variety of environmental conditions. Since the capacity of PV and BESS are different, it is determined that Total Harmonic Distortion (THD) of injected current is high during night mode. To solve this issue and enhance power quality, a double-mode LCL filter is developed. When a single-mode LCL filter is used, the THD value is obtained as 4.8%. In the two-mode LCL filter application, this value has been reduced to 3.2%. The overall efficiency is measured as 97.5% under low irradiation conditions for the system with ANN-MPPT.

**Keywords:** PV, Power quality improvement, ANN MPPT, Energy storage

**Öz**

Teknolojinin hızlı bir şekilde gelişmesine bağlı olarak enerji talebi günden güne artmaktadır. Çevresel talepleri karşılayabilmek için temiz ve sürdürülebilir enerji kaynakları daha yoğun bir şekilde kullanılmalmaktadır. Bu makalede, 12.45 kW Fotovoltaik (FV) sistem ve 10 kWh kapasiteli batarya enerji depolama sisteminden (BEDS) oluşan şebeke bağlantılı bir hibrit sistem tasarlanmıştır. Tasarım prosedüründe Değiştir&Gözle (D&G), Artan İletkenlik (A-İ), Yapay Sinir Ağları (YSA) ve Hibrit Maksimum Güç Noktası İzleme (MGNİ) algoritmaları uygulanmış ve test edilmiştir. Uygulanan algoritmalar arasından değişen çevre koşulları altında FV modülden maksimum güç çıkışını sağlayacak yöntem seçilmiştir. FV ve BEDS'nin güçleri birbirinden farklı olduğu için, sistem gece modundayken Toplam Harmonik Bozulmasının (THB) arttığı tespit edilmiştir. Bu sorunu çözmek ve güç kalitesini arttırmak için iki modlu bir LCL filtresi uygulanmıştır. Tek modlu LCL filter kullanıldığında THD değeri %4.8 elde edilmiştir. İki modlu LCL filter uygulamasında bu değer %3.2'ye düşürülmüştür. Ayrıca YSA- MPPT çalıştırıldığında düşük ışınımda %97.5 sistem verimliliği gözlemlenmiştir.

**Anahtar kelimeler:** FV, Güç kalitesinin iyileştirilmesi, YSA MGNİ, Enerji depolama.

## 1 Introduction

The energy demand is increasing rapidly due to the development of technology, population growth and migration of people to developed countries. To meet this increasing demand, different energy resources are used. The first one is called as conventional resource. It leads to air pollution threatening human health, global warming, melting of glaciers, releasing greenhouse gases, and etc. [1]. In order to cope with these situations, renewable energy sources (RES) offer more environmentally, friendly, reliable, healthy and sustainable energy production way. On a global scale, conventional energy sources are replaced by RES. Recently, technological developments and investments are getting enhanced in this field. Solar energy is very convenient compared with other sources owing to be sustainable, cleaned and abundant [2]. Solar energy is the radiant energy released by the fusion process in the core of the sun. Solar energy can be directly converter into electrical energy with the help of PV panels. The generated voltage and current from the PV vary depending on the irradiance and temperature level. In order to reduce the payback time of the investment costs for PV systems, it is extremely important to keep PV power at maximum level. Various algorithms are used to track the operation point and keep the power at maximum level. These algorithms are called as MPPT methods [3]. MPPT method not only ensures the power maximization from the PV module but also increases the operating life of the PV system [4]. MPPT method basically generates a reference signal. The DC-DC converter is controlled by the Pulse Width Modulation (PWM) signal

* Sorumlu yazar / Corresponding author, e-posta / e-mail: bguzey@hotmail.com (B. Güzey)
Geliş / Recieved: 31.10.2024 Kabul / Accepted: 17.12.2024 Yayımlanma / Published: 15.01.2025
doi: 10.28948/ngumuh.1576914

coming from MPPT integrated controller. The generated control signal is sent to the power converter as a trigger.

This study aims to design a system that enables the transmission of power generated by a PV system to the grid and BESS based on irradiation and temperature levels. When the PV system is off, the system utilizes the BESS to maintain power continuity. BESS is designed to capture energy store for later utilization efficiently. It is crucial to the functioning of electricity. An efficient BESS is significant for enhancing battery performance [5]. In addition to these design objectives, it is aimed to design a single LCL filter that will operate in two separate modes for day and night mode to increase power quality by reducing harmonic distortion of injected current. This design is performed on the MATLAB/Simulink platform. Furthermore, the system should always keep the power produced by the PV panel at a maximum level against changing irradiance levels. It is aimed to use various MPPT algorithms and to determine the most effective one. The response of the system to changing conditions is observed, and a stable system structure is provided

After, this introduction section, in Section 2, the importance and global status of renewable energy, along with the methods for DC-DC converters and MPPT algorithms are presented. In Section 3, the design parameters of the circuit topologies that constitute the system are provided. In Section 4, the results and discussions section compares the outcomes of the applied MPPT methods. Finally, Section 5 presents the overall conclusions of the study.

## 2 Hybrid PV-BESS

In Turkey, energy consumption is rising year by year as shown in Figure 1. Resource utilization is also increasing to meet demand at same ratio. The value and importance of energy resources has increased considerably. Being independent and self-sufficient in the energy sector has become the goal of countries [6]. To meet this demand, RES have taken a crucial role [7]. RES involve solar energy, wind energy, geothermal energy and bioenergy. These resources provide sustainable, reliable, inexhaustible, clean and more technological energy production [8]. According to the EMBER report [9] as shown in Figure 2 solar energy has taken part of 4.5% among whole electricity generation methods in 2022.

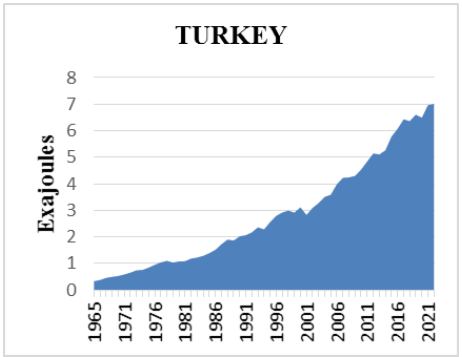


**Figure 1.** Energy consumption graph of Turkey

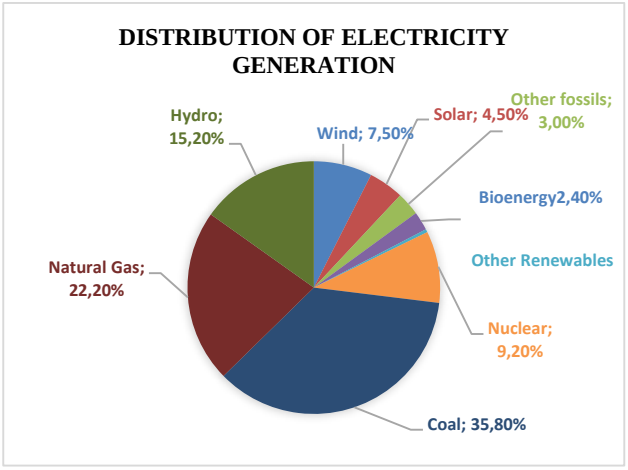


**Figure 2.** Methods of electricity generation in 2022

The irradiation levels of different places are also different. Utilizing solar energy quite descends the negative impact of carbon emissions. Moreover, this type of energy does not release detrimental gases that could devastate the environment. On the other hand, PV panels show that harvesting energy type from the sun is a non-polluting, reliable, and clean source of energy [10]. This source is used either directly or indirectly for various implementations that are not only restricted to industry processes but also feasible in other areas such as the drying of agricultural parts, battery electric vehicles, solar-powered refrigerators, water heating, and solar cooking. Cooking with solar energy can often be used in areas where there is plenty of radiation and no electricity [11]. The producing power from solar is only available in the daytime. If the uninterruptible power generation is required, battery assisted PV systems can be constructed. However, this hybrid systems ensure additional costs that raise the installation cost of the system [12]. PV module efficiencies are generally in the range of 14-22% depending on the quality of the production company. Together with technological developments, the ratio of efficiency is tried to be increased [13]. The temperature factor is also crucial in area selection. The efficiency of PV panels may decrease at high temperatures and this leads to a reduction in energy production [14].

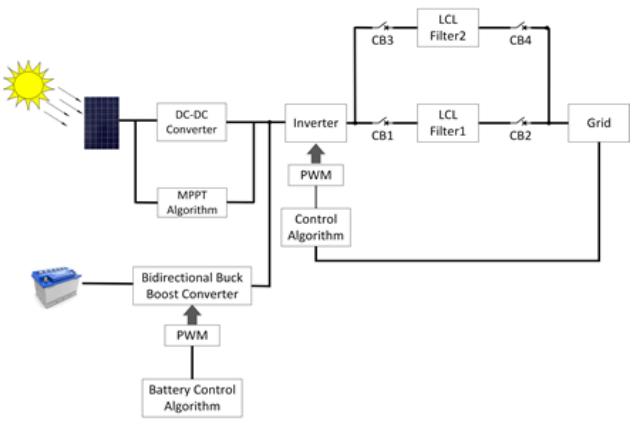


**Figure 3.** Proposed grid-connected hybrid PV&BESS system

The grid-connected hybrid PV & BES system involves PV modules, a DC-DC boost converter, an inverter, an LCL filter, a bidirectional buck-boost converter, and storage units. These are the main parts. DC-DC converters have significant tasks. Adjustment of voltage level and providing operation on maximum power are among these tasks. In many PV applications, the magnitude of voltage on the load side needs to be higher than the generated voltage from PV [15].

### *2.1 DC-DC converter topologies*

A traditional boost converter is comprised of an inductor, a diode, a transistor, and an output capacitor being parallel to the load. The switching devices can be an IGBT or MOSFET [16] as shown in Figure 4.

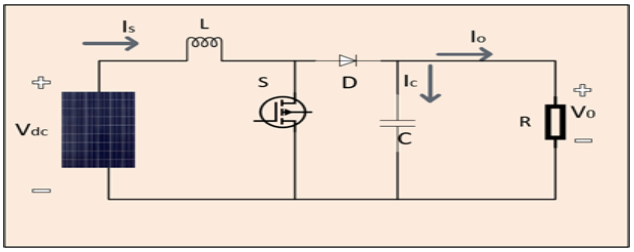


**Figure 4**. Circuit analogy of boost converter

Boost converter can be designed with the following formulas:

$$L = \left(\frac{V_{in}(V_0 - V_{in})}{\Delta I_L * f_s * V_0}\right) \quad (1)$$

$$\Delta I_L = \left(\frac{(0.1) * I_0 * V_0}{V_{in}}\right) \quad (2)$$

$$Duty\ cycle = \left(1 - \frac{V_{in}}{V_0}\right) \quad (3)$$

$$C = (I_0 * Duty\ cycle)/(f_s * V_{oc} * \Delta V_0) \quad (4)$$

$$R = \frac{V_o}{I_0} \quad (5)$$

Another type of converter is the bidirectional buck-boost converter as shown in Figure 5. It can be applied in various applications. As reversed to traditional unidirectional converters, power flows in two directions can be ensured. It can be also used for UPS, fuel cells, wind turbines, photovoltaic systems, plug-in hybrid electric vehicles (PHEV), battery electric vehicles (BEV), and smart grids [17, 18]. Bidirectional arrangements reduce the size of the circuit and increase the performance of the system. There is no need for two converters to adjust the flow of the current in forward and reverse direction. The entire process can be handled in a single circuit. Thus, bidirectional buck-boost converters ensure cost reduction and high reliability for charging batteries [19]. In this paper, a non-isolated bidirectional converter has been used and connected to the battery.

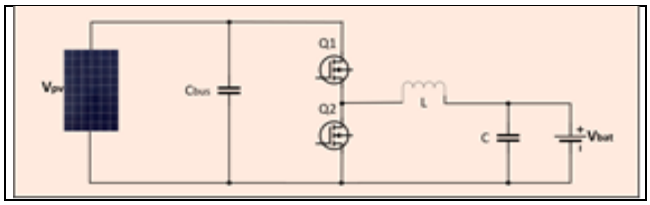


**Figure 5**. Circuit analogy of bidirectional converter

### *2.2 MPPT methods*

In this paper, four different MPPT algorithms are performed. The P&O algorithm is the most common tracking method. The simplicity and low cost of the method make it one of the most preferred techniques. The conventional P&O algorithm has several drawbacks such as convergence speed, determination of accurate perturbation direction, and number of oscillations [20].

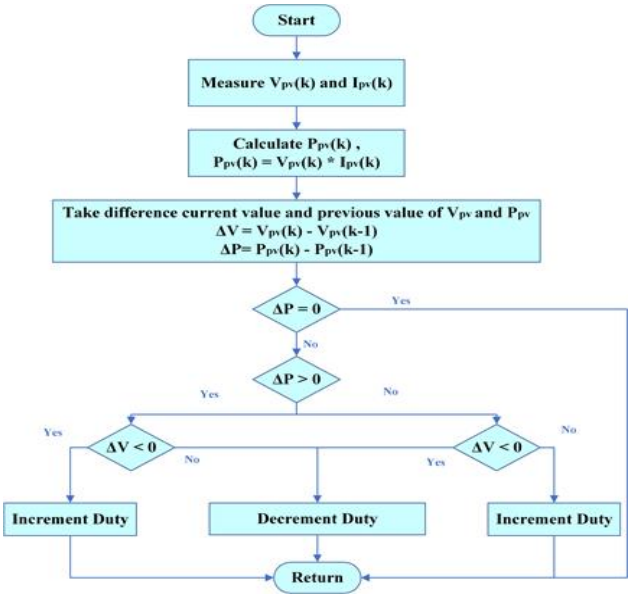


**Figure 6.** Flowchart of P&O algorithm

This topology adjusts the duty ratio by comparing the present value of the power and the previous value. It achieves this by applying a perturbation to the reference. The flowchart of the design is expressed in Figure 6. The topology ensures that the specific parameter stays around the maximum power point by repeatedly perturbing the operating point. If there is a momentary power drop due to changing weather conditions, the P&O algorithm perturbs the reference and adjust the power harvesting level upper position. The second method is called as INC which can eliminate the slow response and steady-state errors of the P&O algorithm. It is advantageous under fast-changing weather conditions due to the dynamic response. However, the INC is more complex and harder to implement than the P&O method. The INC method tracks MPP using the slope of the P-V curve. This procedure uses instantaneous conductance which is represented by I/V and incremental conductance which is symbolized by dI/dV for MPPT [21] and the flowchart is given in Figure 7.

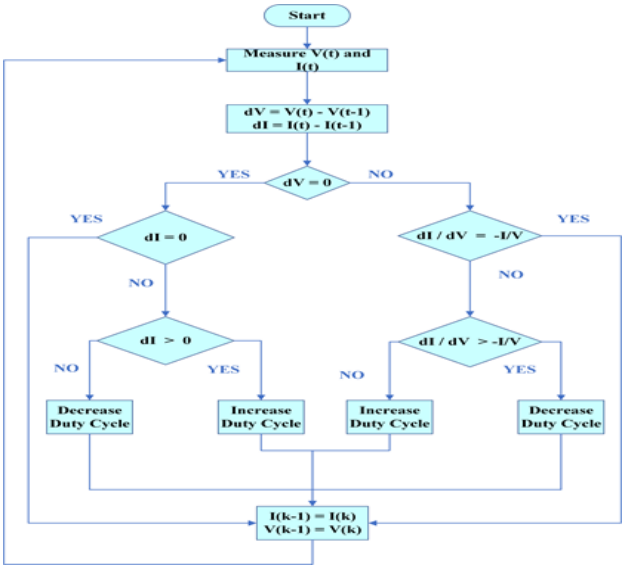


**Figure 7.** Flowchart of INC algorithm

The other method which is called as ANN-MPPT which is an intelligent way to keep the power at maximum level. The response of traditional algorithms is quite low in changing weather conditions. For this reason, traditional methods are replaced with intelligent algorithms. Designing a tracker using an ANN is one of the intelligent ways. ANN-based controllers have several capabilities like nonlinear mapping, robust operation, high-level efficiency, high-speed response [22].

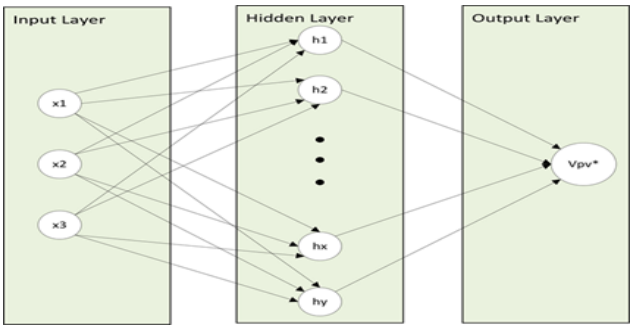


**Figure 8.** Flowchart of ANN algorithm

ANN controller has two inputs which are temperature and irradiance. The aim of the neural network is to arrange the duty ratio for the DC-DC converter. For changes in temperature or irradiation level, the system quickly sets the duty ratio again.

The last method is called as Hybrid-MPPT which is created from the best outputs of three separate methods at certain irradiance levels.

Another special part is the DC/AC inverter in the PV system. Inverters are key components that combine grid and PV circuit design. In a single-stage system, both MPPT and grid synchronization are performed by the inverter [23]. To acquire the best performance from the panel, choosing an appropriate grid-connected inverter is a critical topic [24]. In the design stage of the grid-connected inverters, filters are used for producing pure sine waves. It should be placed between the inverter and the electric grid. The most effective filter to damp the current harmonics is the LCL filter [25]. It can be used at low switching frequencies. It has a lower voltage drop and higher absorption factor compared with conventional L and LC filters [26].

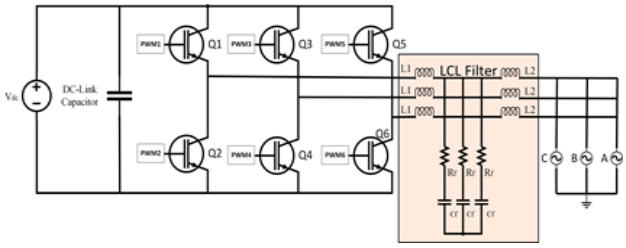


**Figure 9.** Grid-connected inverter with LCL filter

In grid-connected systems, the phase angle information of utility voltage is a crucial part of controlling inverters [27]. Phase information is used in the stage of power control. PLL algorithm acquires this information to synchronize utility and three-phase inverter. The main duty of PLL is to extract phase angles with the help of some specific operations [28]. The performance of the system directly depends on the quality of the PLL design. Besides taking phase information, PLL should provide low distortion output and suppress frequency variations. It includes negative feedback. Thus, the circuit structure becomes a closed loop. It consists of a phase detector, a voltage-controlled oscillator and a loop filter [29].

## 3 Design stage

Panel type and the number of cells differ according to the proposed power level to be produced. In this paper, 1Soltech-1STH-FRL-4H-260-M60 is used as a PV module. The parameters of the PV array are indicated below.

**Table 1.** Parameters of PV system

| | |
|---|---|
| Power at STC (W) | 260 |
| Power at PTC (W) | 231.4 |
| Power Density at STC (W / $m^2$) | 155.689 |
| Vmp: Voltage at Max Power (V) | 31.6 |
| Imp: Current at Max Power (A) | 7.93 |
| Voc: Open Circuit Voltage (V) | 38.6 |
| Isc: Short Circuit Current (A) | 8.21 |
| Open Circuit Voltage Temp Coefficient (%/°C) | -0.356 |
| Short Circuit Current Temp Coefficient (%/°C) | 0.07 |
| Max Power Temp Coefficient (% / °C) | -0.453 |

PV array characteristics are given in Figure 10.

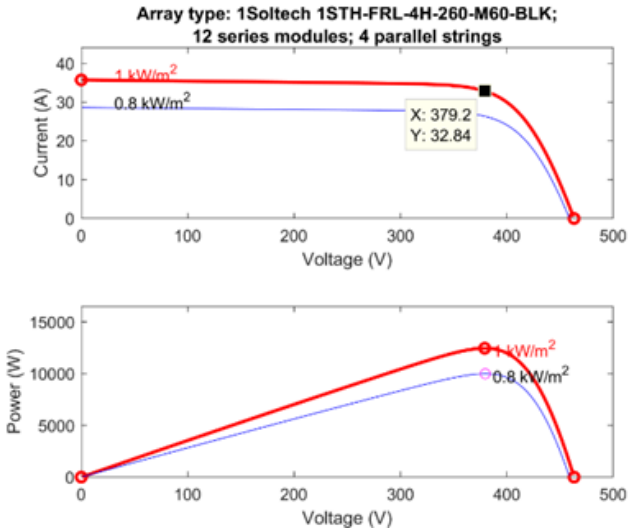


**Figure 10.** The I-V and P-V curves of the PV system

The generated power is transmitted to the boost converter to arrange the power level. The output voltage of the PV panel is about $380V_{dc}$. The system DC bus voltage is calculated as 700V. It is necessary to use a boost converter to increase the voltage level. In addition, current and voltage fluctuations in circuits occur for many reasons. These are called as ripples and to improve system performance, ripple probability should be added to the parameter calculation. The voltage ripple percentage is taken at 1% and the current ripple percentage is taken at 10%. The parameter values of the boost converter are specified in Table 2.

**Table 2.** Boost converter design parameters

| | |
|---|---|
| Input Voltage ($V_{in}$) | 380V |
| Output Voltage ($V_{out}$) | 700V |
| Duty Ratio (D) | 0.4571 |
| Switching Frequency ($f_{sw}$) | 20000Hz |
| Output Current ($I_{out}$) | 17.78A |
| Voltage Ripple (DV) | 7 |
| Current Ripple (DI) | 1.78 |
| Capacitor ($C_{out}$) | 58.076µF |
| Desired Input Current (di) | 3.276A |
| Inductor (L) | 2.6519mH |
| Load (R) | 39.36Ω |

The parameters of DC-DC boost converter is shown in Figure 11. The PWM signal of the boost converter is produced with the help of MPPT algorithms. The efficiency and steady-state response of each algorithm is different.

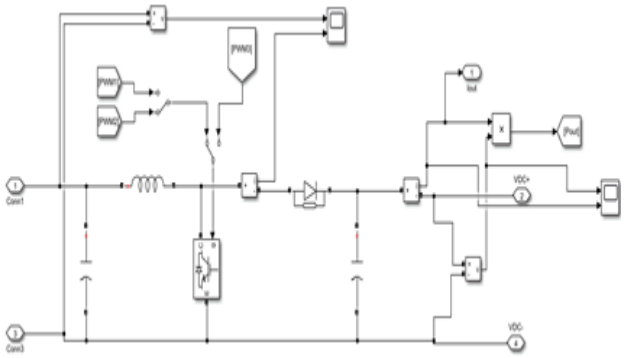

**Figure 11.** Simulation circuit of the boost converter

PWM1 signal is generated using the P&O MPPT method, PWM2 signal is generated using the INC method and PWM3 signal is generated using the ANN method. When these methods are compared, it is determined that different methods provide good reactions for different irradiation levels. For this reason, a hybrid method that combines the best ones in certain irradiances is designed and this system seems more efficient at low radiation levels as shown in Figure 12. After these systems, BESS is performed by combining some different stages. These stages are to build a DC-DC bidirectional buck-boost converter, battery and internal parameters, battery charging, and discharging controller.

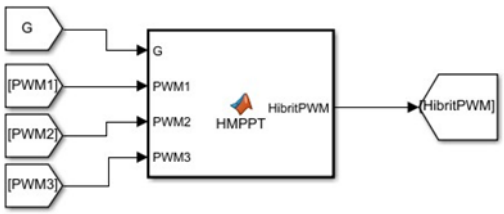


**Figure 12.** Function block of hybrid MPPT

The battery is chosen lithium-ion type. Battery specifications are given in Table 3.

**Table 3.** Design parameters of battery

| | |
|---|---|
| Type of battery | Lithium-Ion |
| Nominal voltage | 420V |
| Rated capacity | 24Ah |
| Cut off voltage | 315V |
| Fully charged voltage | 488.87V |
| Discharge Current | 10.43A |

The designed battery is tied to the DC bus with a bidirectional buck-boost converter that is used to decrease or increase voltage levels during the discharging and charging stages. The device has two sides which are called as high side and the low side. The DC bus voltage is taken at 700V as the high voltage side of the bidirectional converter. Battery voltage is chosen 455V as the low side of the converter. This procedure provides bidirectional current flow. The daytime

period is assumed to be 1 sec. and the nighttime period is assumed to be 1 sec. Since the PV panel generates power during the daytime, the battery performs the charging process. During nighttime, the battery is adjusted to the discharge mode automatically. The circuit diagram is shown in Figure 13 and bidirectional buck-boost converter parameters are stated in Table 4.

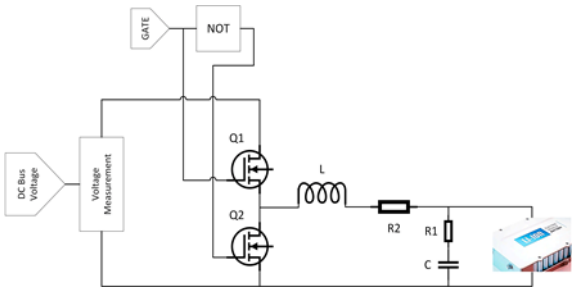


**Figure 13.** Block diagram of BESS

**Table 4.** Parameters of bidirectional converter

| | |
|---|---|
| Capacitor (C) | 1mF |
| First Resistor ($R_1$) | 1Ω |
| Inductor (L) | 6mH |
| Second Resistor ($R_2$) | 0.05Ω |
| DC Bus Voltage ($V_H$) | 700V |
| Battery Voltage ($V_L$) | 455V |
| Switching Frequency | 10kHz |
| Input Current Ripple | 10% |
| Output Current Ripple | 1% |

In the charging state procedure, the difference between the battery voltage and the reference voltage is taken. This obtained value is given to the controller as an input signal. After that, the output of the controller is used to acquire the charging current as shown in Figure 14. The charging operation is assumed as 1 second (between 0 to 1) in the simulation part. The system operates for 1 second in daytime mode and switches to night mode. Another process is called as discharging mode, the difference is taken between the DC bus voltage and the reference voltage.

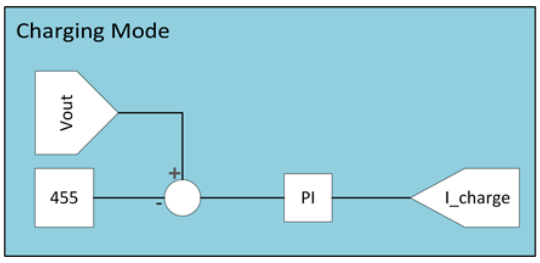


**Figure 14.** Charging controller of BESS

The six separate PWM signals are generated from the incoming signal and given to each switch mode transistor as a trigger signal. p-q control is performed as shown in Figure 15. Park and inverse park transformation is utilized for creating a robust p-q control structure. In addition, phase information is also needed when applying the inverse park transformation which is represented by d-q to a-b-c block in Matlab/Simulink. The phase information component can be easily taken from the PLL circuit performed in the simulation. Since the battery and PV power are different, it is determined that the THD increased in a single LCL filter when switching from day mode and night mode. To prevent this situation, two robust filter modes have been designed according to two separate power levels. During the daytime, the first mode LCL filter works when the PV is in the active region. The second mode, LCL filter is in the off position. During the nighttime, when the PV is cut off region, the second mode LCL filter works.

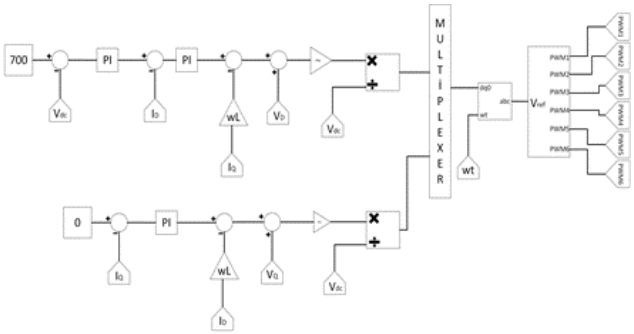


**Figure 15.** Power control of the three-phase inverter

In the first mode, LCL filter is in the off position as shown in Figure 16. The first mode LCL filter corresponds to daytime mode, and the second mode filter is represented to nighttime mode and THD is significantly reduced.

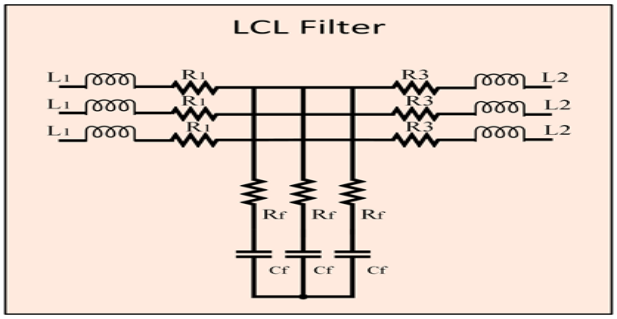


**Figure 16.** Representation of three-phase LCL filter

The parameter values of the first mode LCL filter, referred to as the daytime mode LCL filter, are presented in Table 5. When the PV system is off, the parameter values of the LCL filter are shown in Table 6.

**Table 5.** Daytime mode LCL filter

| | |
|---|---|
| $L_1$ (Left Side Inductor) | 2.5mH |
| $R_1$ (Left Side Resistor) | 1mΩ |
| Capacitor | 22μF |
| $R_f$ (Bottom Side Resistor) | 2Ω |
| $L_2$ (Right Side Inductor) | 100μH |
| $R_3$ (Right Side Resistor) | 1mΩ |

**Table 6.** Nighttime mode LCL filter

| | |
|---|---|
| $L_1$ (Left Side Inductor) | 2.1535mH |
| $R_1$ (Left Side Resistor) | 1mΩ |
| Capacitor | 18.76μF |
| $R_f$ (Bottom Side Resistor) | 0.6286Ω |
| $L_2$ (Right Side Inductor) | 68.85μH |

The two-mode LCL filter, the cost reduction is obtained at 32% on the right-side inductor, 15% on the capacitor, 14% on the left-side inductor, and 31% on the right-side resistor.

## 4 Results of the research

In this section, outcomes of the P&O method at 1000 W/m$^2$ are indicated and the battery is operated for a total of 2 seconds, in daytime mode and nighttime mode. The SOC(%) percentage of the battery, the voltage of the battery, and the battery current value are indicated in Figure 17.

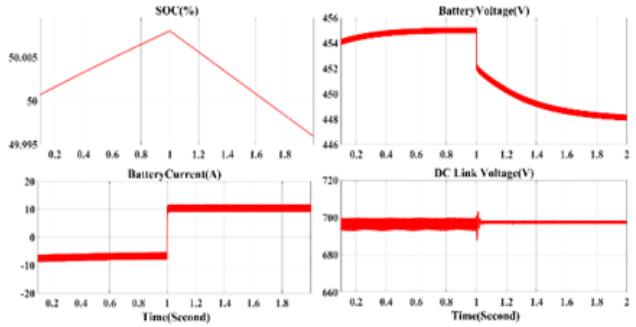


**Figure 17.** Battery outcomes with P&O at 1000 W/m$^2$

At 1000 W/m$^2$ level, the efficiency is around 96% with the P&O method as shown in Figure 18 and Figure 19.

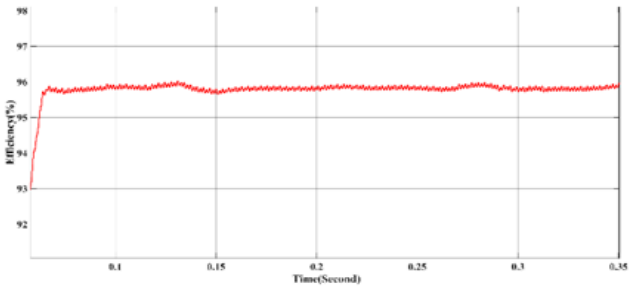


**Figure 18.** Efficiency of P&O method at 1000 W/m$^2$

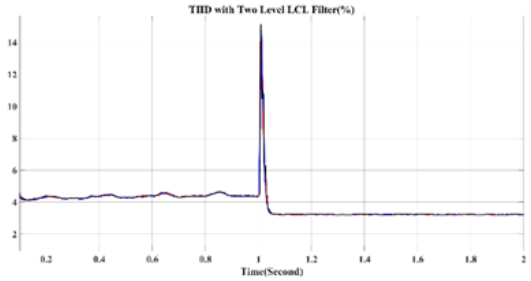


**Figure 19.** THD of two-mode LCL-P&O 1000 W/m$^2$

The outcomes of the battery and DC bus voltage are stated in Figure 20 when INC tracking method is on.

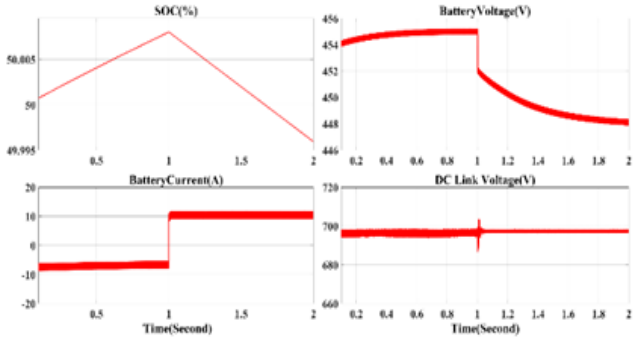


**Figure 20.** Battery outcomes with INC at 1000 W/m$^2$

When the DC bus voltage of the INC method is compared with that of P&O, it is observed that there are fewer ripples in this method as shown in Figure 21. This shows that using the INC method, the pure DC signal form is approached. The efficiency of the INC algorithm is around 95.8%.

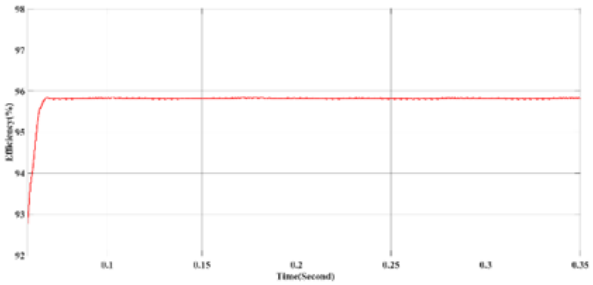


**Figure 21.** Efficiency of INC method at 1000 W/m$^2$

Figure 22 shows the THD graph of the inverter output current. When the system is only in daytime mode, the distortion value decreased compared to P&O while the THD level of the P&O method is between the range of 4.2% - 4.5% in daytime mode. In the INC method, this value is in the range of 4.2% - 4.3%.

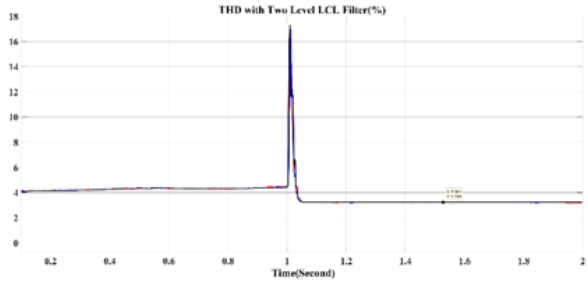


**Figure 22.** THD of two-mode LCL-INC 1000 W/m$^2$

In this part, the ANN tracking method is used at 1000 W/m$^2$. If the DC bus voltage of the ANN method is analyzed as shown in Figure 23, it is observed that there are fewer ripples with using ANN compared to conventional algorithms. The efficiency of the system with ANN method is indicated in Figure 24.

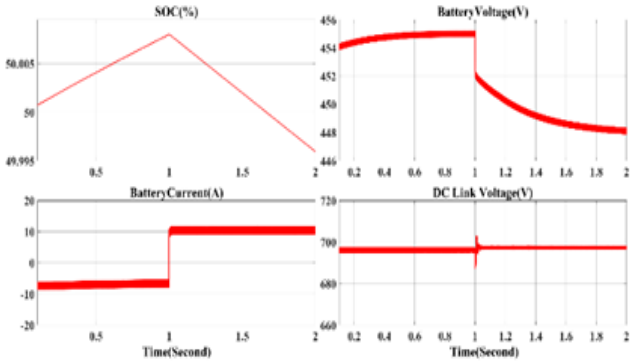


**Figure 23.** Battery outcomes with ANN at 1000 W/m$^2$

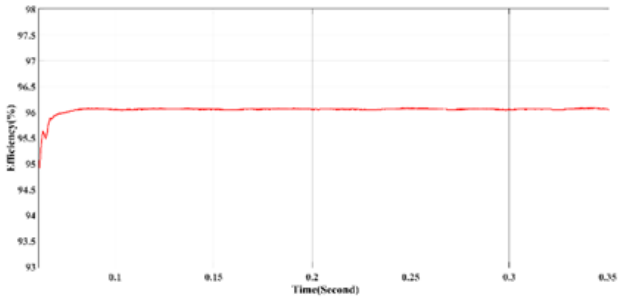


**Figure 24.** Efficiency of ANN method at 1000 W/m$^2$

THD graph of the inverter output current is indicated as shown in In Figure 25. The THD level of the ANN method is between the range of 3.9%- 4% in daytime mode. If the second LCL filter structure is not applied in this circuit, the THD value of the current would have increased up to 5%.

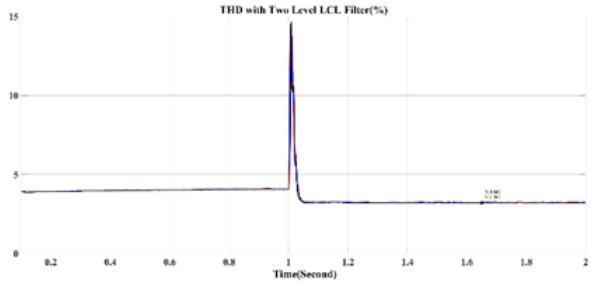


**Figure 25.** THD of two-mode LCL with ANN MPPT at 1000 W/m$^2$

The ANN tracking algorithm is analyzed at 600 W/m$^2$. ANN method gives much smoother inverter output waveform than other methods. The battery and DC bus voltage results are expressed and the battery voltage, current and SOC values are similar to other irradiance levels. The ANN algorithm has a greater effect on DC voltage generation than traditional MPPT methods. The smoothest shape of the DC bus voltage has been acquired in this section by using the ANN based MPPT method at 600 W/m$^2$. The power efficiency of the system at 600 W/m$^2$, which is evaluated as low irradiance is also available in Figure 26. The power efficiency level is achieved around 97.5%. The ANN tracking method gives more efficient results and THD level at low irradiation as shown in Figure 27. The distortion value during daytime mode is between 2.95% - 3.05% which is the best THD acquired in daytime mode as shown in Figure 28.

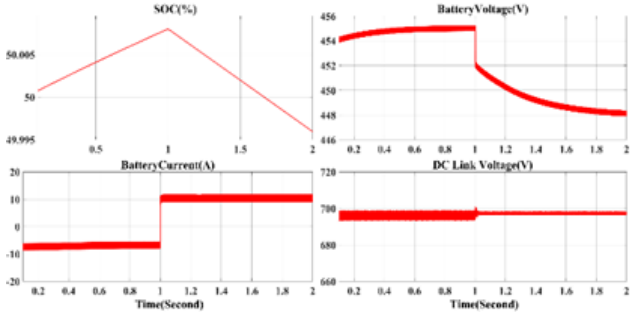


**Figure 26.** Battery outcomes with ANN at 600 W/m$^2$

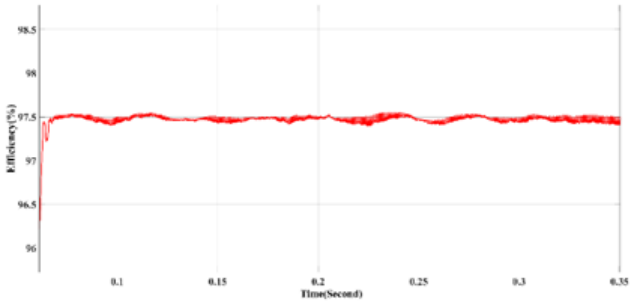


**Figure 27.** Efficiency of ANN method at 600 W/m$^2$

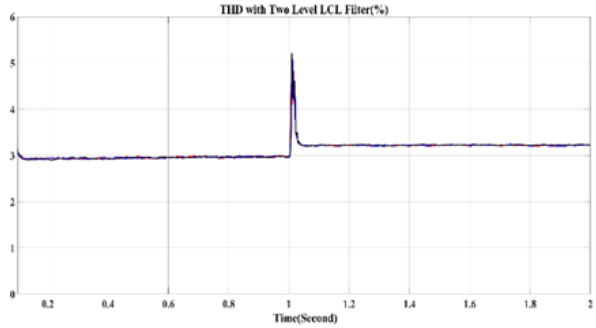


**Figure 28.** THD of two-mode LCL-ANN 600 W/m$^2$

All the previous simulation results are evaluated and efficiency levels are studied. The percentage of efficiency offered by each method is different when the irradiance level changes. The obtained graph for specific irradiance is also available in Figure 29 and 30. The values alter from 1000 W/m$^2$ to 0 W/m$^2$ during the interval of 0-1 second. The irradiance parameter starts from 1000 W/m$^2$ and then it decreases to 800 W/m$^2$ at 0.2 seconds. After the change of selected MPPT during 0.2 to 0.4 seconds, the radiation level brings down from 800 W/m$^2$ to 600 W/m$^2$ at 0.4 seconds. Then, the efficiency percentage of an MPPT method is determined for 600 W/m$^2$ is between 0.4 to 0.6 seconds. When the simulation time is at 0.6 seconds, the irradiance level is reduced to 400 W/m$^2$. The selected MPPT for 400 W/m$^2$ is executed for 0.2 seconds. When the simulation time reaches 0.8s, the radiation level is decreased to 200 W/m$^2$.

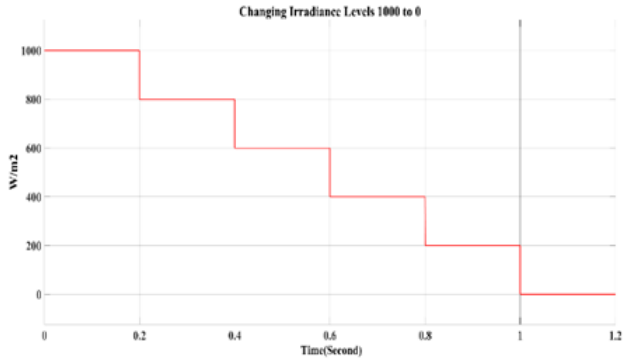


**Figure 29.** Irradiance level for hybrid-MPPT

PWM produced by P&O-MPPT is used at 1000 W/m$^2$. When the radiation level reaches 800 W/m$^2$, all algorithms are compared and it is observed that the most efficient method is INC. All the results for 600 W/m$^2$ are examined and the most efficient method becomes ANN- MPPT. For the 400 W/m$^2$, ANN gives the most efficient result. Finally, the 200 W/m$^2$ INC algorithm ensures the best outcome.

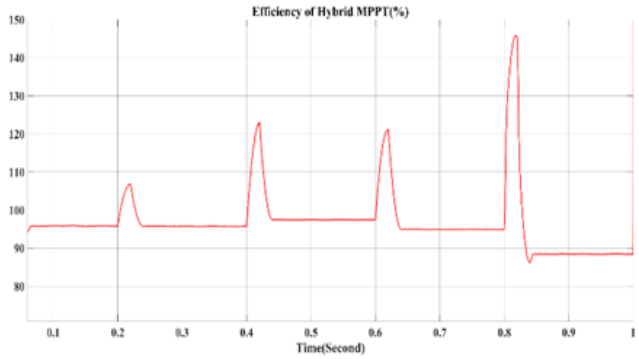


**Figure 30.** Efficiency result of hybrid mode MPPT

The efficiency and THD values are stated in Table 7.

**Table 7.** Summary of simulation results

| General Simulation Outcomes of Paper | | | | | | |
|---|---|---|---|---|---|---|
| | P&O | | INC | | ANN | |
| Irr. (W/m$^2$) | Thd (%) | Eff. (%) | Thd (%) | Eff. (%) | Thd. (%) | Eff. (%) |
| 1000 | 4.03 | 95.8 | 4.11 | 95.8 | 3.9 | 96 |
| 800 | 3.42 | 95.5 | 3.51 | 95.7 | 3.3 | 97.6 |
| 600 | 2.95 | 95.2 | 3.08 | 95.2 | 2.9 | 97.4 |
| 400 | 3.01 | 93.5 | 2.76 | 93.7 | 2.5 | 94.9 |
| 200 | 2.54 | 87.4 | 2.42 | 88.5 | 2.3 | 86.7 |

## 5 Conclusions

The main objective of this paper is to determine the algorithm that keeps the energy obtained from sunlight at the maximum level in the most efficient way. The power generated by the PV panel is studied at three irradiance levels: 1000 W/m², 800 W/m², and 600 W/m². These irradiance levels are tested with three different MPPT methods, excluding the hybrid method. In the hybrid method, irradiance levels range from 1000 W/m² to 200 W/m². The system operates in daytime mode between 0-1 seconds. During this time, the PV feeds the battery and transfers power to the grid. In the time interval of 1-2 seconds, the PV enters the cut-off region, and the battery switches to discharge mode to supply power to the system. The initially designed single-mode LCL filter resulted in high THD during the transition from daytime to nighttime, so efforts were focused on addressing this issue. The high THD is caused by the difference between the power produced by the PV and the power supplied by the battery. To overcome this problem, two-mode LCL filter that operates separately for daytime and nighttime is used. When the PV is active, the first mode filter operates, and the second mode filter is off. When the PV is inactive, the first filter turns off, and the second filter becomes active. A new improvement to the LCL filter contributes to a decrease in THD from 4.8% to 3.2%. The algorithm that provides the best results at low irradiance levels is the Hybrid MPPT method. In this tracking algorithm, PWM is generated with ANN at low irradiance levels. At high irradiance levels, conventional methods are used to generate PWM. Maximum efficiency of 97.5% - 97.7% is achieved using the ANN algorithm. In recent studies, the importance and implementation of hybrid energy solutions continue to increase day by day [30-34].

### Conflict of interest

Authors declare that there is no conflict of interest.

**Similarity rate (iThenticate):** 11 %

### References

[1] B. Guzey, Design and power quality improvement of a grid connected hybrid pv system. MsC Thesis, Cukurova University, Adana, Turkey, 2023.

[2] T. T. E. Vo, H. Ko, J. Huh, and N. Park, Overview of solar energy for aquaculture: the potential and Future Trends. Energies, 14(21): 6923-6943, 2021. https://doi.org/10.3390/en14216923

[3] A. S. Eldessouky, I. M. Mahmoud, and T. S. Abdel-Salam, Mppt based on a novel load segmentations structure for pv applications. Ain Shams Engineering Journal, 14(4): 101937-101949, 2023. https://doi.org/10.1016/j.asej.2022.101937

[4] A. R. Reisi, M. H. Moradi, and S. Jamasb, Classification and comparison of maximum power point tracking techniques for photovoltaic system: a review. Renewable and Sustainable Energy Reviews, 19(1):433-443,2013. http://dx.doi.org/10.1016/j.rser.2012.11.052

[5] S. Nyamathulla, C. Dhanamjayulu, A review of battery energy storage systems and advances battery management system for different applications: challenges and recommendations. Journal of Energy Storage, 86(1): 111179, 2024. https://doi.org/10.1016/j.est.2024.111179

[6] M. P. Randelovic, N. Kocic, and B. S. Randelovic, The importance of renewable energy sources for sustainable development. Economics and Sustainable Development, 4(2): 15-24, 2020. http://dx.doi.org/10.5937/ESD2002016P

[7] Y. Yalman, Ö. Çelik, A. Tan, K. Ç. Bayindir, Ü. Çetinkaya, M. Yeşil, and B. Khan, Impacts of large-

scale offshore wind power plants integration on Turkish power system. IEEE access, 10(1), 83265-83280, 2022. https://doi.org/10.1109/ACCESS.2022.3196779

[8] I. Hussein, Ö. Çelik, A. Teke, A hybrid random parameters modification to mppt algorithm to mitigate interharmonics from single-phase grid-connected PV systems. Energy Reports, 8, 6234-6244, 2022. https://doi.org/10.1016/j.egyr.2022.04.062

[9] Ember, Global Electricity Review 2023. Clean energy policy and data, 762–769, 2023.

[10] Ö, Çelik, K. Zor, A. Tan, A. Teke, A novel gene expression programming-based mppt technique for PV micro-inverter applications under fast-changing atmospheric conditions. Solar Energy, 239, 268-282, 2022. http://dx.doi.org/10.1016/j.solener.2022.05.012

[11] S. K. Sansaniwal, V. Sharma, and J. Mathur, Energy and exergy analyses of various typical solar energy applications: a comprehensive review. Renewable and Sustainable Energy Reviews, 82(1): 1576-1601, 2018. https://doi.org/10.1016/j.rser.2017.07.003

[12] Solar Energy Research. https://understandsolar.com/advantagesvs-disadvantages-solar-power/ Accessed 05 October 2024

[13] M. S. Abd-Elhady, M. M. Fouad, and T. Khalil, Improving the efficiency of photovoltaic (pv) panels by oil coating. Energy Conv. and Management, 115(1): 1-7, 2016. https://doi.org/10.1016/j.enconman.2016.02.040

[14] K. A. Moharram, M. S. Abd-Elhady, H. A. Kandil, and H. El-Sherif, Enhancing the performance of photovoltaic panels by water cooling. Ain Shams Engineering Journal, 4(4): 869-877, 2013. https://doi.org/ 10.1016/j.asej.2013.03.005

[15] R. R. Gopi, and S. Sreejith, Converter topologies in photovoltaic applications – a review. Renewable and Sustainable Energy Reviews, 94(1):1-14, 2018. https://doi.org/10.1016/j.rser.2018.05.047

[16] M. F. Adnan, M. A. M. Oninda, M. M. Nishat, and N. Islam, Design and simulation of a dc-dc boost converter with pid controller for enhanced performance. International Journal of Engineering Research & Technology (IJERT), 6(9):1-6, 2017. http://dx.doi.org/10.17577/IJERTV6IS090029

[17] O. Onar, J. Kobayashi, D. C. Erb, and A. Khaligh, A bidirectional high-power-quality grid interface with a novel bidirectional noninverted buck-boost converter for phevs. IEEE Transactions on Vehicular Technology, 61(5): 2018-2032, 2012. https://doi.org/10.1109/TVT.2012.2192459

[18] Z. Zhang, and K. T. Chau, Pulse-width-modulation-based electromagnetic interference mitigation of bidirectional grid-connected converters for electric vehicles. IEEE Transactions on Smart Grid, 8(6): 2803-2812, 2017. https://doi.org/10.1109/TSG.2016.2541163

[19] S. A. Gorji, H. G. Sahebi, M. Ektesabi, and A. B. Rad, Topologies and control schemes of bidirectional dc-dc power converters: an overview. IEEE Access, 7(1): 117997-118019, 2019. https://doi.org/10.1109/ACCESS.2019.2937239

[20] L. Shang, H. Guo, and W. Zhu, An improved mppt control strategy based on incremental conductance algorithm. Protection and Control of Modern Power Systems, 5(14): 1-8, 2020. https://doi.org/10.1186/s41601-020-00161-z

[21] R. Alik, A. Jusoh, and T. Sutikno, A review on perturb and observe maximum power point tracking in photovoltaic system. TELEKOMNIKA, 13(3): 745-751, 2015. http://doi.org/10.12928/telkomnika.v13i3.1439

[22] Ö. Çelik, and A. Teke, A hybrid mppt method for grid connected photovoltaic systems under rapidly changing atmospheric conditions. Electric Power Systems Research, 152, 194-210, 2017. https://doi.org/10.1016/j.epsr.2017.07.011

[23] J. Khan, and H. M. Arsalan, Solar power technologies for sustainable electricity generation – a review. Renewable and Sustainable Energy Reviews, 55(1): 414-425, 2016. https://doi.org/10.1016/j.rser.2015.10.135

[24] D. Kolantla, S. Mikkili, S. R. Pendem, and A. A. Desai, Critical review on various inverter topologies for pv system architectures. The Institution of Engineering of Technology Journals (IET) Renewable Power Generation, 14(17): 3418-3438, 2020. https://doi.org/10.1049/iet-rpg.2020.0317

[25] N. Yu, J. Yang, S. Chen, and M. Ye, Design of lcl-filter based three-level active power filters. Indonesian Journal of Electrical Engineering, 12(1): 48-56, 2014. http://dx.doi.org/10.11591/telkomnika.v12i1.3441

[26] M. Dursun, and M. K. Döşoğlu, Lcl filter design for grid connected three-phase inverter. 2018 Second International Symposium on Multidisciplinary Studies and Innovative Technologies (ISMSIT), 2018. http://doi.org/10.1109/ISMSIT.2018.8567054

[27] V. Kaura, and V. Blasko, Operation of a phase locked loop system under distorted utility conditions. IEEE Transactions on Industry Applications, 33(1): 58-63, 1997. https://doi.org/10.1109/28.567077

[28] S,Golestan, J. M. Guerrero, J. C. Vasquez, 2017. Three-phase plls: a review of recent advances. IEEE Transactions on Power Electronics, 32(3): 1894-1907, 2017. https://doi.org/10.1109/TPEL.2016.2565642

[29] S. R. Nandukar, M. Rajeev, Design and simulation of three phase inverter for grid connected photovoltaic systems. Proceedings of Third Biennial National Conference (NCTE), 2012.

[30] L. Abdolmaleki, U. Berardi, Hybrid solar energy systems with hydrogen and electrical energy storage for a single house and a midrise apartment in North America, International Journal of Hydrogen Energy, 52(2): 1381-1394, 2024. https://doi.org/10.1016/j.ijhydene. 2023.11.222

[31] M. K. Khan, M. Raza, M. Shahbaz, U. Farooq, M. U. Akram, Recent advancement in energy storage technologies and their applications, Journal of Energy Storage, 92, 112112, 2024

https://doi.org/10.1016/j.est.2024.112112
[32] B. Li, Z. Liu, Y. Wu, P. Wang, R. Liu, L. Zhang, Review on photovoltaic with battery energy storage system for power supply to buildings: challenges and opportunities, Journal of Energy Storage, 61, 106763, 2023. https://doi.org/10.1016/j.est.2023.106763
[33] A. Khazali, Y. Al-Wreikat, E. J. Fraser, S. M. Sharkh, A. J. Cruden, M. Naderi, M. J. Smith, D. Palmer, D. T. Gladwin, M. P. Foster, et al. Planning a hybrid battery energy storage system for supplying electric vehicle charging station microgrids. Energies, 2024; 17(15):3631. https://doi.org/10.3390/en17153631
[34] W. Jan, A. D. Khan, and M. Z. Abbasi, A comprehensive review of hybrid photovoltaic-battery systems: Evaluating progress, identifying key issues, and exploring future prospects in sustainable energy integration. Appl. Photovol. Tech., vol. 1, no. 1, Jan. 2024. https://doi.org/10.59400/apt.v1i1.320